LIÈGE université

MEASUREMENTS AND CORRELATION OF TIMOLOL MALEATE SOLUBILITY IN BIOBASED NEAT AND BINARY SOLVENT MIXTURES

Lennart Zimmermann[1], Hung Lin Lee[2], Aibolat Koishybay[3], Cornelis P. Vlaar[4], Jean-Christophe M. Monbaliu[5], Rodolfo J. Romañach[6], Md. Noor-E-Alam[7], Allan S. Myerson[8], and Torsten Stelzer[9]*

[1]*Department of Chemical Engineering, Massachusetts Institute of Technology, Cambridge, Massachusetts 02139, United States; Bioseparation Engineering Group, Technical University of Munich, Garching D-85748, Germany;* ⊙ *orcid.org/0009-0009-5009-1987*

[2]*Department of Chemical Engineering, Massachusetts Institute of Technology, Cambridge, Massachusetts 02139, United States;* ⊙ *orcid.org/0000-0001-9931-8083*

[3]*Department of Chemical Engineering, Massachusetts Institute of Technology, Cambridge, Massachusetts 02139, United States;* ⊙ *orcid.org/0009-0007-1184-6457*

[4]*Department of Pharmaceutical Sciences, University of Puerto Rico − Medical Sciences Campus, San Juan, Puerto Rico 00936, United States;* ⊙ *orcid.org/0000-0001-5145-8300*

[5]*Center for Integrated Technology and Organic Synthesis, MolSys Research Unit, University of Liège B-4000 Liège (Sart Tilman), Belgium;* ⊙ *orcid.org/0000-0001-6916-8846*

[6]*Department of Chemistry, University of Puerto Rico − Mayagüez, Mayagüez, Puerto Rico 00681, United States;* ⊙ *orcid.org/0000-0001-7513-7261*

[7]*Department of Mechanical and Industrial Engineering, College of Engineering, Center for Health Policy and Healthcare Research, Northeastern University, Boston, Massachusetts 02115, United States;* ⊙ *orcid.org/0000-0001-5353-9710*

[8]*Department of Chemical Engineering, Massachusetts Institute of Technology, Cambridge, Massachusetts 02139, United States;* ⊙ *orcid.org/0000-0002-7468-8093*

[9]Department of Chemical Engineering, Massachusetts Institute of Technology, Cambridge, Massachusetts 02139, United States; Department of Pharmaceutical Sciences, University of Puerto Rico − Medical Sciences Campus, San Juan, Puerto Rico 00936, United States; Crystallization Design Institute, Molecular Sciences Research Center, University of Puerto Rico, San Juan, Puerto Rico 00926, United States; ⊙ *orcid.org/0000-0003-3881-0183; Email: torsten.stelzer@upr.edu*

ABSTRACT

A crucial factor in the development of sustainable crystallization processes is the use of biobased solvents, which, in turn, necessitates a comprehensive understanding of the solubility profiles of solid compounds in biobased solvents. The solubility of timolol maleate (TIM), used to treat glaucoma, was measured in commercial biobased solvents at temperatures ranging from 278.15 to 333.15 K using the polythermal method. Its solubility was determined in eight neat biobased solvents (acetone, 1-butanol, Cyrene, dimethyl isosorbide (DMI), ethanol, 2-methyltetrahydrofuran (2-MeTHF), 2-propanol, and water) and three binary solvent mixtures (ethanol + 2-propanol, ethanol + 2- MeTHF, and ethanol + DMI). It was demonstrated that the solubility of TIM increases with temperature in the pure solvents

and solvent mixtures. Furthermore, the solubility of TIM decreases in ethanol with increasing 2-propanol, 2-MeTHF, or DMI content, which may act as antisolvents. The experimental solubility data of TIM in the pure solvents and binary solvent mixtures were correlated using the modified Apelblat, Yaws, and λh equations. The correlated solubility data agree well with the experimental results, indicated by the small relative deviation and average relative deviation (ARD %) values. The correlated and experimentally determined solubility data provide crucial information for the design of sustainable crystallization processes for TIM.
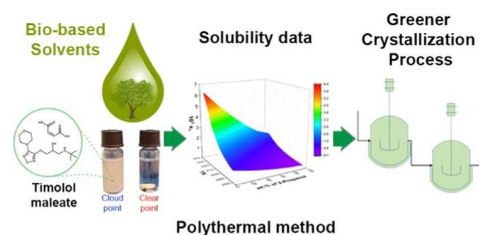
Introduction

Solvents are key elements of chemical processes that provide a suitable medium for synthetic reactions,[1] liquid–liquid extraction,[2] chromatography,[3] and crystallization for separation and purification of compounds.[1,4–6] For chemical manufacturing, including active pharmaceutical ingredients (APIs), solvents constitute about 80% of the total chemicals used.[7] Therefore, using biobased solvents, derived from biorenewable resources or extracted from biomass, is recognized as one of the key opportunities toward sustainability.[5] Driven by global initiatives to stimulate sustainable manufacturing toward a bioeconomy,[8–10] the principles of green chemistry[11] and green engineering[12] are gaining more attention to minimize the dependence on fossil fuels and improve the environmental and health impacts of chemical manufacturing.[12,13] As a result, there is a growing demand for the development of sustainable manufacturing of high-value-added chemicals from biobased and renewable feedstocks, including APIs.[13–15] To achieve truly sustainable pharmaceutical manufacturing, the processes for molecule generation (synthesis) and separation/purification (crystallization) need to be integrated into an uninterrupted processing network.[16,17] For the development of crystallization processes, solubility data play an essential role because about 90% of all APIs require at least one crystallization step.[18] To advance the sustainability of pharmaceutical manufacturing, the availability of solubility data of APIs in biobased solvents is becoming increasingly important. To date, published solubility data of APIs in biobased solvents is scarce. Only a few reports on phase equilibria studies have been documented for extraction [19,20] and carbon capture processes.[21] Thus, there is a need to report and document solubility data of biobased solvents in academia and industry to promote sustainable process development with reduced environmental impact. Additionally, the reporting of any form of solubility data is sustainable in itself as it reduces the resource input required for solubility determination by other research groups working on the same compound.

First approved in 1978, timolol maleate (TIM) is an essential medicine to treat glaucoma.[22,23] The S-enantiomer of TIM (Figure 1) is pharmacologically active as a nonspecific β-adrenergic blocker, while the R-enantiomer is almost inactive.[24] Though the free base form timolol hemihydrate (trade name Betimol) possesses similar biological activities compared to its salt form timolol maleate (TIM),[25,26] generally, the salt form of APIs have enhanced aqueous solubility and stability desired for the commercial formulations[27,28] and is assumed to be true for TIM under the trade names Istalol and Timoptic. To the best of our knowledge, the only reported crystal structures of TIM to date are the commercially enantiopure (*S*)-TIM and the racemic (*R*,*S*)TIM (CSD codes: TIMOLM01 and FALPEP, respectively).[29]

Figure 1.
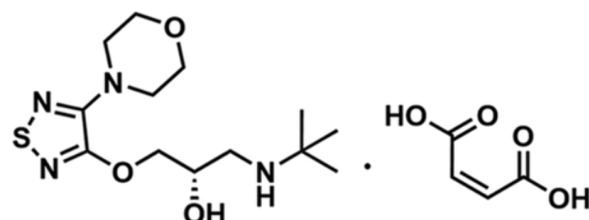
Molecular structure of *S*-timolol maleate (TIM)

Upon reviewing the available literature, the information available on reported solubility data for TIM is very limited.[30,31] Therefore, the present study focuses on the determination of the solubility of TIM in eight commercially available biobased neat solvents (acetone, 1-butanol, Cyrene, dimethyl isosorbide (DMI), ethanol, 2-methyltetrahydrofuran (2-MeTHF), 2-propanol, and water), and three binary solvent mixtures (ethanol +2-propanol, ethanol + 2-MeTHF, and ethanol + DMI) at temperatures ranging from 278.15 to 333.15 K using the polythermal method in a Crystal16 parallel crystallization system.[32–37] All solvents are biobased and classified by the Food & Drug Administration as Class 3 solvents[38] or recommended to be listed as Class 3 (Table 1).[39–41] Class 3 solvents are less toxic and of lower risk to human health.[38] Moreover, the solvents listed in Table 1 are, to our knowledge, the only biobased solvents commercially available from common vendors.

The experimentally determined solubility data for TIM were correlated employing the modified Apelblat, Yaws, and λh equations to enable both interpolation and extrapolation of these data to understand the physicochemical properties.[42–45] Thus, the solubility data presented in this study offer pathways to engineering sustainable crystallization processes for TIM for advanced and greener pharmaceutical manufacturing.

Experimental Section

MATERIALS.

Table 1 summarizes the CAS number, supplier, purity (as provided by the vendor), and analytical method for the solute and solvents used in this study. All solvents used for the solubility measurements were from biorenewable sources as certified by the vendor. They are all categorized as Class 3 solvents[38] or are recommended to be listed as Class 3.[39–41] In addition, diethylamine, hexane, methylene chloride, 2-propanol (all HPLC-grade), and a certified reference material of Timolol-related compound A [(*R*)-TIM] were used for the analysis of the enantiomeric purity of TIM.[46] Micropurified water was obtained using a Barnstead MicroPure UV/UF purification system (Thermo Scientific, 18.20 MΩ/cm, pH = 7.03, mV = −42.0). All materials were used "as received" without further purification.

Table 1. *Mass Fraction Purities of the Solutes and Solvents Used in This Study with the Corresponding Analytical Methods and Suppliers*

chemical name	CAS number	supplier	purity (%)[a]	purification method	analysis method	solvent classification[38,41]
timolol maleate (TIM)	26921-17-5	RIA International	99.8	none	HPLC[d]	
timolol-related compound A	26839-77-0	Sigma-Aldrich	95.4	none	HPLC	
acetone[b]	67-64-1	Sigma-Aldrich	≥99.5	none	GC[e]	class 3
1-butanol[c]	71-36-3	Sigma-Aldrich	≥99.7	none	GC[e]	class 3
cyrene[b]	53716-82-8	Sigma-Aldrich	98.7	none	GC[e]	class 3[g]
diethylamine	109-89-7	Sigma-Aldrich	≥99.5	none	GC[e]/MS[f]	
dimethyl isosorbide (DMI)[b]	5306-85-4	Sigma-Aldrich	≥99.0	none	GC[e]	class 3[g]
ethanol (200 proof)[b]	64-17-5	Sigma-Aldrich	≥99.5	none	GC[e]	class 3
hexane	110-54-3	Sigma-Aldrich	≥95.0	none	HPLC[d]	class 2
methylene chloride	75-09-2	Supelco	≥99.9	none	GC[e]	class 2
2-methyltetrahydrofuran (2-MeTHF)[b]	96-47-9	Sigma-Aldrich	≥99.0	none	GC[e]	class 3[g]
2-propanol[b]	67-63-0	Sigma-Aldrich	≥99.5	none	GC[e]	class 3

[a]Provided by suppliers. [b]Vendor-certified biobased solvents. [c]Commercially available biobased solvent but back-ordered by all known vendors. Therefore, a petro-based solvent was used instead. [d]High-performance liquid chromatography. [e]Gas chromatography. [f]Mass spectroscopy. [g]This solvent has been recommended to be listed as Class 3.[41]

SOLUBILITY MEASUREMENTS.

The polythermal method was used to determine the solubility of TIM (1) in all neat solvents (acetone, 1-butanol, Cyrene, DMI, ethanol, 2-propanol, and water), except 2-MeTHF, and all three binary solvent mixtures [ethanol (2) + 2-propanol (3), ethanol (2) + 2-MeTHF (3), and ethanol (2) + DMI (3)]. The polythermal method is a proven and validated approach that determines the temperature at which a solute is dissolved with a known concentration at a constant heating rate using an automated multiple reactor system (Crystal16, Technobis Crystallization Systems).[34−37,47] Suspensions were prepared by precisely weighing the solute TIM and one of the solvents or solvent mixtures for predetermined concentrations into 2 mL sealed glass vials (Agilent Technologies) using two analytical balances with a precision of ±0.1 mg (XS104 and MS104S, Mettler Toledo). The suspensions were stirred using magnetic stir bars (rare earth, 8 × 3 mm^2, Fisherbrand) at 700 rpm while heating from 278.15 to 333.15 at 0.3 K/min. For acetone, the temperature range was adjusted to 278.15–323.15 K because of its low boiling point at 329.15 K.[48] Assuming that dissolution kinetics can be neglected,[49] the temperature at which a

solution is free of crystals and thus saturated was determined as a clear point or saturated temperature upon heating by monitoring the transmission of light through the suspensions from the Crystallization Systems software (version 2.0.3.2860).[33] An isothermal method was used to determine the solubility of TIM in 2-MeTHF via the gravimetric approach in at least quintuplate ($n \geq 5$).[50,51] Briefly, excess solids of TIM were suspended in 3 mL of 2-MeTHF in 8 mL sealed glass vials (Chemglass Life Sciences) maintained at predefined temperatures between 293.15 and 333.15 K under stirring at 700 rpm for ≥72 h using an automated multiple reactor system (Crystalline, Technobis Crystallization Systems). Thereafter, the stirring was halted to allow the solids to settle before withdrawing 0.6 mL of the supernatant quickly filtered with 25 mm PTFE syringe filters (0.2 μm pore size, VWR International) into preweighed vials. The total weight of the vials kept at 60 °C under reduced pressure (ADP31, Yamato Scientific American Inc.) was frequently measured using an analytical balance (XS104, Mettler Toledo) until their weight remained unchanged. The uncertainty of the saturation temperature measurements is within ±0.1 K. The mole fraction solubility (x_i) of TIM was calculated using eq 1.

$$x_i \frac{m_i/M_i}{\sum_{i=1}^{n} m_i/M_i} \tag{1}$$

In eq 1, m_i and M_i, respectively, represent the mass (g) and molecular weight (g/mol) of component i, which is the solute TIM, neat solvents, or solvent mixtures in this study. The molecular weight of TIM is 432.49 g/mol,[31] and the ones used for the neat solvents are obtained as provided by suppliers.

POWDER X-RAY DIFFRACTION (PXRD).

PXRD was performed using a PANalytical X'Pert Pro MPD diffractometer equipped with a Cu Kα source ($\lambda = 1.5419$ Å) and a nickel filter, operated at a voltage of 45 kV and a current of 20 mA with an X'Celerator RTMS detector in scanning mode. Diffractograms were collected over the 2ϑ range 4–41° at a step size of 0.0167° with a rate of 59.69 s/step. The solid form of "as received" TIM was determined prior to the solubility measurements (Figure S12). The resulting suspensions after the completed solubility experiments were filtered by using a polyethylene-frit filter funnel with a pore size of 10 μm (OptiCHEM) to collect solids for the determination of their solid phase.

HIGH-PERFORMANCE LIQUID CHROMATOGRAPHY (HPLC).

To determine the enantiomeric purity of TIM, an HPLC method was adopted from the US Pharmacopeia (USP) with a slight modification in the mobile phase.[46] Briefly, the HPLC analysis was performed by injecting 5 μL into an Agilent 1260 Infinity system equipped with a chiral column (Chiralcel ODH, 4.6 × 250 mm², 5 μm), kept at room temperature, and a UV detector (297 nm). The mobile phase composed of diethylamine, 2-propanol, and hexane (0.5:40:960 v/v/v) was pumped at a constant flow rate of 1 mL/min. While a higher diethylamine content (2:40:960 v/v/v) was reported in the USP monograph,[46] the adjustment was needed to minimize the fluctuations in the pressure and UV baselines at the higher content observed in the HPLC system used in this study. Preliminary tests have shown that in the

modified method, both TIM enantiomers can still be resolved with retention times matching the ones reported in the USP (Figure S11).[46] TIM "as received" and the solid materials collected after the completed solubility experiments were dissolved in a diluent that was made of methylene chloride and 2-propanol (25:75 v/ v) to achieve a target concentration of 1 mg/mL.[46]

DIFFERENTIAL SCANNING CALORIMETRY (DSC).

A DSC (Q2000, TA Instruments) equipped with an RC40 singlestage refrigeration unit was used to determine the onset melting temperature ($T_{m,\,onset}$) of "as received" TIM. The instrument was calibrated using indium as a standard (T_m = 429.62 K and ΔH_{fus} = 28.8 J/g). Samples (~0.9 ± 0.1 mg) of TIM were weighed using an analytical balance (XS104, Mettler Toledo) and placed on a Tzero aluminum pan (TA Instruments) that was then hermetically sealed. The samples were equilibrated at 313.15 K for 10 min before heating to 523.15 K at a rate of 10 K/min (temperature accuracy of 0.1 K) under a nitrogen purge (50 mL/min). DSC measurements were conducted five times (n = 5) and analyzed employing TA Universal Analysis 2000 software (version 4.5A) to obtain an accurate average $T_{m,\,onset}$.

THERMOGRAVIMETRIC ANALYSIS (TGA).

TGA (Q5000, TA Instruments) was used to record the change in the weight of TIM as a function of temperature. The instrument was calibrated by using calcium oxalate monohydrate as a standard. Samples (~6 ± 0.5 mg) were equilibrated at 313.15 K for 10 min before heating to 523.15 K at a rate of 10 K/min (temperature accuracy of 0.1 K) under a nitrogen purge of 50 mL/min. The TGA thermograms of five samples (n = 5) were analyzed using TA Universal Analysis 2000 software (version 4.5A).

Thermodynamic Models

The experimentally determined solubility data were correlated with three frequently employed thermodynamic models, namely, the modified Apelblat, Yaws, and λh equations, to describe solid–liquid equilibrium relationships or solubility behavior of solutes in both neat solvents and solvent mixtures.[42−45] These correlations allow us to interpolate and extrapolate the solubility data of TIM over a broad range of temperatures and provide a better understanding and interpretation of the solution behavior of TIM in the biobased solvents and solvent mixtures.[36,43−45]

MODIFIED APELBLAT EQUATION.

The modified Apelblat equation (eq 2) is a widely used semiempirical model to correlate the solubility of a solute as a function of temperature.[34,36,42,43,52,53]

$$\ln x_1 = A_1 + \frac{B_1}{T} + C_1 \ln T \tag{2}$$

In eq 2, x_1 is the mole fraction solubility of TIM, T is the absolute temperature in Kelvin (K), and A_1, B_1, and C_1 are the empirical model parameters. The values of A_1 and B_1 represent the variations in the solubility activity coefficient, whereas the value of C_1 reflects the effect of temperature, T, on the enthalpy of fusion.[42,54] The Apelblat equation parameters are given a subscript 1 to distinguish them from Yaws' equation parameters (eq 3).

YAWS EQUATION.

The semiempirical Yaws equation (eq 3), first proposed by Yaws[55] to correlate the solubility of hydrocarbons in water, has been widely applied to correlate the solubility of various solutes in monosolvents[56–59] and binary solvent mixtures.[60]

$$\ln x_1 = A_2 + \frac{B_2}{T} + \frac{C_2}{T^2}$$

(3)

Similar to eq 2, in eq 3, x_1 represents the mole fraction solubility of TIM, T is the absolute temperature in Kelvin (K), and A_2, B_2, and C_2 are the empirical model parameters. The Yaws equation parameters are given a subscript 2 to distinguish them from the modified Apelblat equation parameters in eq 2.

λh EQUATION.

The λh equation (eq 4), first proposed by Buchowski et al.,[61] is frequently used to correlate the mole fraction solubility, x_1, of a solute with temperature in a solid– liquid equilibrium system.[34,42,43,52,53] It can be expressed as[59]

$$\ln \left[1 + \lambda \frac{1-x_1}{x_1}\right] = \lambda h \left(\frac{1}{T} - \frac{1}{T_m}\right)$$

(4)

where x_1 represents the mole fraction solubility of TIM and T and T_m are the experimental and normal melting temperatures of TIM in Kelvin (K), respectively. The model parameters, λ and h, are associated with the nonideal properties of the solution and the excess mixture enthalpy of the solution, respectively.

Data correlations utilizing the modified Apelblat, Yaws, and λh equations were performed by using the software OriginPro 2023b (OriginLab Corporation, version 10.0.5.157). The Levenberg–Marquardt Algorithm was applied to solve the fitting problem for nonlinear curves. The correlations between the experimental and calculated solubility data were evaluated by calculating the relative deviation (RD) and the percent average relative deviation (ARD %) based on eqs 5 and 6, respectively.

$$RD_i = \frac{x_{1,i}^{exp} - x_{1,i}^{cal}}{x_{1,i}^{exp}}$$

(5)

$$ARD\% = \frac{100}{N} \sum_{i=1}^{N} \left|\frac{x_{1,i}^{exp} - x_{1,i}^{cal}}{x_{1,i}^{exp}}\right|$$

(6)

In eqs 5 and 6, N is the total number of experiments, while $x^{exp}_{1,i}$ and $x^{cal}_{1,i}$ are the ith experimental and calculated mole fraction solubility, respectively.

RESULTS AND DISCUSSION

VALIDATION OF THE HEATING RATE EMPLOYED IN THE POLYTHERMAL METHOD.

To ensure that the experimentally determined solubility data was measured accurately, the solubility of TIM in ethanol was measured at different heating rates of 0.1, 0.2, and 0.3 K/min in the temperature range from 279.1 to 329.8 K (Figure 2).[34,36] Since explicit solubility data of TIM are not reported in the literature (only one vague value at "room temperature" without providing a quantifiable temperature),[30] it was decided to utilize the solubility measured in ethanol at 0.1 K/min as the reference ($RD_{0.1 \text{ K/min}}$ = 0) for the calculation of the average RD of the experimentally determined saturation temperatures at the faster heating rates. The average RD was used to maintain a positive or negative impact compared to ARD %.[34–37] Figure 2 shows that the average RDs of the saturated temperature for each concentration data point negligibly deviate around the null value (Table S2). Specifically, the average RDs for 0.2 and 0.3 K/min are $RD_{0.2 \text{ K/min}}$ = 0.034 and $RD_{0.3 \text{ K/min}}$ = 0.194, respectively, indicating that the measurements using both heating rates have reached quasi-solid–liquid equilibrium conditions.[34] Consequently, the heating rate of 0.3 K/min was used for all further experiments because similar accuracy could be achieved in a shorter time compared to the measurements using the heating rates of 0.1 and 0.2 K/min.[34,36,37,62,63]

To further evaluate the accuracy of the applied polythermal method, the solubility of TIM in the neat solvent water was compared with the only available data point documented in the literature using an isothermal method (Table S3). Unfortunately, the reported solubility for TIM is not clearly stated with regard to the temperature. Specifically, Gaikwad et al.[30] reported the solubility at rather vaguely "room temperature", without providing an exact temperature value. Thus, it was assumed that the room temperature was between 288.15 and 298.15 K according to the definition of the European Pharmacopeia,[64] when TIM was dissolved in water with occasional shaking of the vial for 24 h.[30] In addition, the supernatant was analyzed by offline UV spectrophotometry without detailed information on sample preparation.[30] This leaves room for various uncertainties regarding the assessment of the reported solubility. Yet, the solubility of TIM in water determined in this study (x_1 = 0.00255 at 288.15 K and x_1 = 0.00299 at 298.15 K), calculated using the modified Apelblat equation, are in a similar order of magnitude compared with the one reported in the literature (x_1 = 0.00363 at room temperature).[30]

Figure 2.
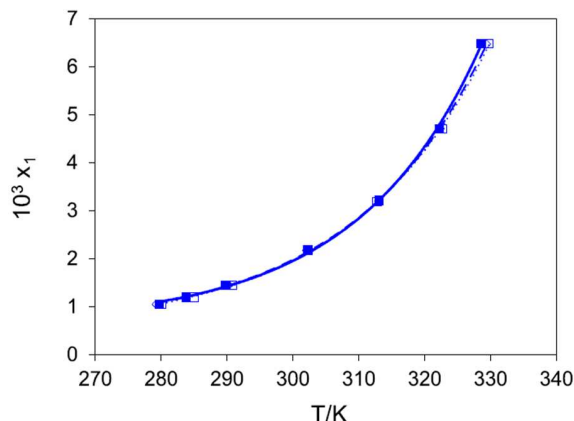
Experimental and correlated solubility of TIM in ethanol at different heating rates: blue square solid, 0.1 K/min; blue diamond open, 0.2 K/min; and blue square open, 0.3 K/min. The trendlines are calculated using the modified Apelblat equation.

THERMAL ANALYSIS OF TIM.

Thermodynamic data for TIM were not available in the literature. Thus, the ΔH_{fus} and $T_{m, onset}$ values of TIM were determined experimentally in this study. DSC and TGA data and their representative thermographs are provided in Table S1 and Figure S1, respectively. The average onset melting temperature, $T_{m, onset}$, was 476.79 ± 0.10 K, while the average ΔH_{fus} value was 57.7 ± 4.0 kJ/mol. To convert the unit from J/g to kJ/mol for ΔH_{fus}, the measured enthalpy of fusion was multiplied by the molecular weight (MW) of TIM (MW = 432.49 g/mol) and then divided by 1000 (see the Supporting Information). The TGA thermographs reveal that the decomposition of TIM starts at 470.25 K, which is below the average $T_{m, onset}$ of 476.79 K, as determined by DSC. Though the average decomposition of TIM at the heating rate of 10 K/min is ≤7.1%, it makes the determination of thermodynamic properties, e.g., melting temperature, inaccurate or even impossible.[65] The melting temperature of TIM is a parameter in the λh equation (eq 4).[61] Though it is generally preferred to measure melting temperatures at slow heating rates for accuracy,[65] the use of faster rates is an acceptable method to avoid decomposition during melting point determination.[66] In an attempt to identify a heating rate that would result in $T_{m, onset}$ of TIM before its decomposition temperature ($T_{decomp, onset}$), different heating rates were tested (Figure S2). An exponential regression (best possible fit) of the data reveals that the use of a heating rate of >62 K/min would be theoretically necessary to achieve a complete melting of TIM before $T_{decomp, onset}$. The achievable heating rate for the conventional DSC employed in this study is ≤50 K/min.[67,68] Therefore, the $T_{m, onset}$ for TIM could not reliably be determined in this study, impacting the calculation of x_1^{cal} using the λh equation. Though it was not accessible for this study, a fast-scan DSC might be utilized to determine the melting point of TIM without thermal decomposition occurring before and during the melting.[65] The fast-scanning rates (several hundred K/min) of samples ≤100 μg in such a DSC would effectively push possible decomposition to higher temperatures and away from, e.g., melting, sublimation, and evaporation.[66]

Table 2. *Experimental and Correlated Mole Fraction Solubility (x_1) of TIM (1) in Neat Solvents at Different Temperatures (T) and at Ambient Pressure p = 101.3 kPa[a]*

		Apelblat		Yaws				Apelblat		Yaws	
T (K)	$10^3 x_1^{exp}$	$10^3 x_1^{cal}$	10^2 RD	$10^3 x_1^{cal}$	10^2 RD	T (K)	$10^3 x_1^{exp}$	$10^3 x_1^{cal}$	10^2 RD	$10^3 x_1^{cal}$	10^2 RD
		Acetone						1-Butanol[b]			
281.1	0.48	0.47	2.21	0.47	2.08	278.3	0.28	0.30	-7.03	0.30	-7.68
288.3	0.56	0.58	-2.70	0.58	-2.65	281.7	0.34	0.33	1.61	0.34	1.41
292.8	0.65	0.66	-1.37	0.66	-1.30	284.8	0.38	0.38	1.62	0.38	1.66
301.9	0.89	0.87	2.46	0.87	2.48	289.6	0.49	0.45	7.40	0.45	7.64
313.3	1.21	1.22	-0.86	1.23	-0.91	303.2	0.75	0.79	-6.61	0.79	-6.40
323.1	1.66	1.65	0.13	1.65	0.14	305.1	0.87	0.86	0.43	0.86	0.58
						309.1	1.02	1.03	-0.47	1.03	-0.42
						316.3	1.44	1.42	2.03	1.42	1.94
						321.4	1.78	1.79	-0.17	1.79	-0.28
						328.7	2.51	2.51	-0.16	2.51	-0.12
		Cyrene						DMI			
284.0	0.47	0.56	-18.58	0.560	-18.24	282.6	0.22	0.27	-20.27	0.26	-15.57
286.1	0.54	0.63	-16.03	0.63	-15.76	289.1	0.34	0.34	0.65	0.34	2.13
289.8	0.75	0.77	-1.63	0.77	-1.48	297.5	0.52	0.46	10.43	0.47	9.90
292.4	1.00	0.88	11.91	0.88	12.00	309.7	0.72	0.71	1.50	0.72	-0.19
301.1	1.46	1.36	6.39	1.36	6.37	325.9	1.17	1.24	-6.05	1.24	-6.45
312.2	2.30	2.31	-0.60	2.32	-0.69	330.9	1.51	1.47	3.01	1.46	3.53
323.7	3.79	3.86	-1.78	3.86	-1.84						
332.0	5.50	5.47	0.58	5.47	0.61						
		Ethanol						2-MeTHF			
280.1	1.05	1.06	-0.53	1.06	-1.02	293.2	0.10	0.09	10.79	0.10	1.92
285.0	1.20	1.21	-1.09	1.21	-1.05	303.2	0.17	0.18	-6.73	0.18	-9.85
290.8	1.45	1.45	-0.10	1.44	0.23	313.2	0.38	0.36	5.97	0.35	6.39
302.3	2.17	2.14	1.51	2.13	1.76	323.2	0.67	0.69	-3.09	0.68	-1.92
312.8	3.19	3.17	0.38	3.18	0.32	333.2	1.30	1.30	0.27	1.30	0.27
322.7	4.71	4.76	-0.94	4.76	-1.09						
329.8	6.48	6.46	0.30	6.45	0.36						
		2-Propanol						Water			
279.5	0.13	0.12	1.74	0.12	1.29	286.0	2.45	2.50	-1.93	2.50	-2.16
282.9	0.14	0.15	-2.88	0.15	-3.06	293.1	2.77	2.73	1.31	2.72	1.56
290.9	0.18	0.21	-20.93	0.21	-20.72	300.5	3.19	3.14	1.34	3.14	1.56
293.6	0.25	0.24	1.08	0.24	1.28	305.0	3.52	3.50	0.64	3.50	0.73
298.8	0.37	0.31	15.87	0.31	16.05	313.9	4.49	4.53	-0.96	4.54	-1.14
313.7	0.60	0.64	-7.30	0.64	-7.33	320.8	5.72	5.75	-0.50	5.76	-0.69
321.7	0.97	0.95	2.40	0.95	2.32	325.8	6.94	6.96	-0.29	6.96	-0.28
330.1	1.43	1.43	-0.24	1.43	-0.21	327.2	7.40	7.36	0.56	7.35	0.67

[a]Standard uncertainties, *u*, are $u(T)$ = 2 K. Relative uncertainties, u_r, are $u_r(p)$ = 0.1, $u_r(x_1)$ = 0.04. x_1^{exp} refers to the experimental mole fraction solubility. x_1^{cal} refers to the calculated solubility data applying the modified Apelblat and Yaws equations. RD represents the respective relative deviation. [b]Petro-based 1-butanol is used because the biobased solvent is back-ordered by all known vendors.

SOLUBILITY DATA.

Tables 2, 3, 4, and 5 summarize the experimentally measured and correlated mole fraction solubility (x_1) of TIM (1) in both the biobased neat and binary solvents, together with the RD. The solubility of TIM (1) in the eight neat solvents (acetone, 1-butanol, Cyrene, DMI, ethanol, 2-MeTHF, 2-propanol, and

water), correlated using the modified Apelblat and Yaws equations, is given in Table 2. The solubility of TIM (1) in the binary solvent mixtures ethanol (2) + 2-propanol (3), ethanol (2) + 2MeTHF (3), and ethanol (2) + DMI (3), correlated using the modified Apelblat and Yaws equations, is given in Tables 3, 4, and 5, respectively. Considering the decomposition of TIM (≤7.1%) at $T_{m, onset}$, the correlated solubility of TIM in the neat solvent and binary solvent mixtures employing the λh equation are presented in Tables S4–S7 for comparison.

Table 3. *Experimental and Correlated Mole Fraction Solubility of TIM (x 1) in Ethanol (2) + 2-Propanol (3) at Different Temperatures (T) and at Ambient Pressure p = 101.3 kPa[a]*

		Apelblat		Yaws				Apelblat		Yaws	
T (K)	$10^3 x_1^{exp}$	$10^3 x_1^{cal}$	10^2 RD	$10^3 x_1^{cal}$	10^2 RD	T (K)	$10^3 x_1^{exp}$	$10^3 x_1^{cal}$	10^2 RD	$10^3 x_1^{cal}$	10^2 RD
		W_3=0.20						W_3=0.40			
280.4	0.75	0.76	-1.17	0.77	-1.60	282.4	0.55	0.55	-0.95	-1.42	0.55
284.1	0.85	0.85	-0.03	0.85	-0.08	288.8	0.66	0.68	-2.56	-2.44	0.68
289.1	1.01	1.00	0.53	1.00	0.76	299.3	1.00	0.99	1.43	1.72	0.99
300.3	1.47	1.48	-0.84	1.48	-0.60	304.6	1.23	1.21	1.33	1.52	1.21
304.7	1.77	1.74	1.48	1.74	1.61	314.7	1.84	1.83	0.52	0.44	1.83
314.1	2.52	2.52	-0.04	2.52	-0.14	324.7	2.79	2.82	-1.20	-1.35	2.82
323.3	3.66	3.68	-0.51	3.69	-0.64	331.7	3.88	3.87	0.38	0.44	3.86
329.7	4.86	4.85	0.19	4.85	0.26						
		W_3=0.60						W_3=0.80			
281.2	0.34	0.34	0.34	0.35	-0.08	283.6	0.20	0.22	-6.63	-6.97	0.22
285.1	0.41	0.40	2.11	0.40	2.01	286.7	0.24	0.25	-5.37	-5.44	0.25
291.5	0.49	0.51	-5.79	0.51	-5.61	288.5	0.28	0.27	4.98	5.03	0.27
296.3	0.61	0.63	-2.21	0.62	-1.99	294.8	0.36	0.35	2.28	2.53	0.35
303.0	0.86	0.83	4.42	0.82	4.56	305.8	0.60	0.58	2.53	2.70	0.58
313.8	1.32	1.31	0.75	1.31	0.70	315.4	0.89	0.91	-1.51	-1.54	0.91
323.4	1.96	1.99	-1.46	1.99	-1.56	324.9	1.43	1.43	-0.09	-0.19	1.43
330.5	2.74	2.73	0.42	2.73	0.47	332.2	2.04	2.03	0.11	0.15	2.03

[a]Standard uncertainties, u, are $u(T)$ = 2 K. Relative uncertainties, u_r, are $u_r(p)$ = 0.1, $u_r(x_1)$ = 0.04, $u_r(w_3)$ = 0.00003. x_1^{exp} refers to the experimental mole fraction solubility. x_1^{cal} refers to the calculated solubility data applying the modified Apelblat and Yaws equations. RD represents the respective relative deviation. w_3 reflects the mass fraction of 2-propanol (3) in the binary ethanol (2) + 2-propanol (3) solvent mixture.

Table 4. *Experimental and Correlated Mole Fraction Solubility of TIM (x_1) in Ethanol (2) + 2-MeTHF (3) at Different Temperatures (T) and at Ambient Pressure p = 101.3 kPa[a]*

		Apelblat		Yaws				Apelblat		Yaws	
T (K)	$10^3 x_1^{exp}$	$10^3 x_1^{cal}$	10^2 RD	$10^3 x_1^{cal}$	10^2 RD	T (K)	$10^3 x_1^{exp}$	$10^3 x_1^{cal}$	10^2 RD	$10^3 x_1^{cal}$	10^2 RD
		W_3=0.22						W_3=0.42			
283.6	1.24	1.23	0.39	1.23	0.09	284.6	1.21	1.23	-1.63	-1.81	1.23
289.4	1.44	1.45	-1.01	1.45	-0.93	295.5	1.69	1.66	2.32	2.49	1.65
294.4	1.68	1.69	-0.52	1.69	-0.32	302.5	2.02	2.04	-0.78	-0.67	2.04
304.4	2.39	2.35	1.51	2.35	1.62	312.0	2.76	2.76	0.06	0.01	2.76
314.1	3.30	3.31	-0.35	3.31	-0.42	322.6	3.94	3.96	-0.35	-0.45	3.96
322.8	4.57	4.59	-0.35	4.59	-0.44	328.5	4.89	4.89	0.17	0.23	4.88
328.6	5.75	5.75	0.17	5.74	0.22						
		W_3=0.62						W_3=0.81			
280.0	0.81	0.79	1.95	0.80	1.68	283.4	0.44	0.44	-0.19	0.44	-0.45
285.2	0.88	0.90	-2.37	0.90	-2.33	289.7	0.50	0.50	-0.70	0.50	-0.65
291.7	1.05	1.06	-0.57	1.06	-0.39	292.4	0.53	0.53	0.61	0.53	0.72
299.8	1.33	1.31	1.15	1.31	1.28	296.9	0.59	0.59	0.69	0.59	0.83
307.8	1.65	1.65	-0.20	1.65	-0.21	305.6	0.73	0.73	0.32	0.73	0.37
317.3	2.19	2.20	-0.06	2.20	-0.18	314.4	0.91	0.92	-1.61	0.92	-1.68
327.7	3.04	3.04	0.01	3.04	0.04	323.5	1.21	1.19	1.20	1.19	1.13
						329.7	1.42	1.43	-0.37	1.43	-0.32

[a]Standard uncertainties, u, are $u(T)$ = 2 K. Relative uncertainties, u_r are $u_r(p)$ = 0.1, $u_r(x_1)$ = 0.04, $u_r(w_3)$ = 0.00003. x_1^{exp} refers to the experimental mole fraction solubility. x_1^{cal} refers to the calculated solubility data applying the modified Apelblat and Yaws equations. RD represents the respective relative deviation. w_3 reflects the mass fraction of 2-MeTHF (3) in the binary ethanol (2) + 2-MeTHF (3) solvent mixture.

Table 5. *Experimental and Correlated Mole Fraction Solubility of TIM (x_1) in Ethanol (2) + DMI (3) at Different Temperatures (T) and at Ambient Pressure p = 101.3 kPa[a]*

		Apelblat		Yaws				Apelblat		Yaws	
T (K)	$10^3 x_1^{exp}$	$10^3 x_1^{cal}$	10^2 RD	$10^3 x_1^{cal}$	10^2 RD	T (K)	$10^3 x_1^{exp}$	$10^3 x_1^{cal}$	10^2 RD	$10^3 x_1^{cal}$	10^2 RD
		W_3=0.27						W_3=0.49			
284.0	2.05	2.00	2.37	2.01	2.10	286.2	2.53	2.56	-1.13	2.57	-1.34
289.2	2.28	2.33	-1.87	2.33	-1.85	295.4	3.39	3.34	1.32	3.34	1.42
299.8	3.20	3.21	-0.49	3.21	-0.33	301.0	4.00	3.96	1.01	3.96	1.12
304.6	3.74	3.74	-0.01	3.74	0.09	308.2	4.90	4.96	-1.34	4.96	-1.30
312.8	4.88	4.91	-0.50	4.91	-0.52	320.4	7.33	7.38	-0.66	7.38	-0.73
319.5	6.22	6.16	0.84	6.17	0.77	326.6	9.20	9.08	1.29	9.09	1.26
328.7	8.50	8.51	-0.21	8.51	-0.19	330.3	10.24	10.30	-0.60	10.30	-0.56
		W_3=0.70						W_3=0.86			
281.7	2.1	2.10	-0.24	2.11	-0.47	290.0	1.37	1.40	-2.37	1.40	-2.35
286.9	2.36	2.37	-0.25	2.37	-0.20	302.8	2.06	1.99	3.45	1.99	3.50
290.9	2.63	2.61	0.60	2.61	0.74	310.9	2.50	2.48	0.62	2.48	0.61
300.9	3.39	3.38	0.16	3.38	0.28	316.6	2.82	2.91	-3.14	2.91	-3.18
308.8	4.19	4.21	-0.44	4.21	-0.45	325.1	3.72	3.68	1.05	3.68	1.02
319.0	5.69	5.68	0.18	5.69	0.07	330.1	4.23	4.23	-0.11	4.23	-0.08
328.3	7.56	7.56	-0.03	7.56	0.01						

[a]Standard uncertainties, u, are $u(T)$ = 2 K. Relative uncertainties, u_r, are $u_r(p)$ = 0.1, $u_r(x_1)$ = 0.04, $u_r(w_3)$ = 0.00003. x_1^{exp} refers to the experimental mole fraction solubility. x_1^{cal} refers to the calculated solubility data applying the modified Apelblat and Yaws equations. RD represents the respective relative deviation. w_3 reflects the mass fraction of DMI (3) in the binary ethanol (2) + DMI (3) solvent mixture.

Table 6. *Optimized Correlation Parameters of the Modified Apelblat and Yaws Equations Used to Correlate the Mole Fraction Solubility of TIM (1) in all Neat and Binary Solvent Mixtures and Their ARD %*

	Apelblat				Yaws			
			model					
solvent	A_1	B_1	C_1	ARD % [a]	A_2	B_2	C_2	ARD % [a]
acetone	-142.8206	3771.4206	21.5897	0.0220	12.9953	-9348.5913	995 401.9989	0.0251
1-butanol	-300.4316	9893.1201	45.6158	0.1343	29.2709	-18 118.5791	216 452.3969	0.1682
cyrene	-3.0677	-3958.0087	1.6852	2.4689	8.7568	-4769.3777	44 313.7223	2.3793
DMI	-95.5939	1215.4990	14.7191	1.7893	9.6018	-7084.6760	578 499.9009	1.6681
ethanol	-357.6178	13 029.5131	53.9917	0.0661	32.6862	-20 163.0138	2 546 232.0322	0.0685
2-MeTHF	-92.0784	-1710.6764	15.5918	1.4405	32.5285	-18 942.5460	1 962 933.4958	0.6401
2-propanol	-207.9785	5243.1233	31.9942	1.2829	23.4216	-14497.6109	1519 948.2952	1.2981
water	-582.1048	24 121.0503	86.9474	0.0217	46.2526	-29 232.8811	4 087 410.5450	0.0309
			Ethanol (2) + 2-Propanol (3)[b]					
$w_3 = 0.20$	-324.3405	11 424.8528	49.0432	0.0822	30.1445	-18 697.4656	2 308 691.3492	0.0979
$w_3 = 0.40$	-338.7216	11 948.6612	51.1947	0.1507	31.6664	-19 712.6884	2 443 539.8803	0.1551
$w_3 = 0.60$	-247.7363	7583.7680	37.7353	0.1773	25.1821	-15 697.3819	1792 569.1114	0.1884
$w_3 = 0.80$	-268.2378	8198.3892	40.8843	0.4606	27.7158	-17 185.6948	1 966 726.0549	0.4659
			Ethanol (2) + 2-MeTHF (3)[c]					
$w_3 = 0.22$	-298.2544	10 568.3465	45.1152	0.0222	27.4637	-17 222.6260	2 136 934.5395	0.0231
$w_3 = 0.42$	-279.7530	9938.6708	42.1394	0.0342	24.8620	-15 966.1578	1 987 848.5321	0.0336
$w_3 = 0.62$	-227.7724	7769.2643	34.2313	0.0127	19.4915	-13 158.3039	1596 710.1616	0.0161
$w_3 = 0.81$	-230.7580	8112.9706	34.4249	0.0056	18.1666	-13 096.0387	1 631 062.2530	0.0062
			Ethanol (2) + DMI (3)[d]					
$w_3 = 0.27$	-232.5574	7735.8596	35.2465	0.0190	22.4109	-14 043.1964	1 679 873.9495	0.0090
$w_3 = 0.49$	-212.5045	6918.6045	32.2387	0.0146	20.7928	-13 056.7703	1 545 169.3519	0.0181
$w_3 = 0.70$	-229.0476	7943.5641	34.5135	0.0019	20.3519	-13 216.7862	1619 203.5195	0.0029
$w_3 = 0.86$	-127.1874	3320.3952	19.2546	0.0854	12.0652	-8557.0639	914 591.3597	0.0794

[a]ARD % is the percentage average relative deviation between experimental and calculated values. [b]w_3 reflects the mass fraction of 2-propanol (3) in the binary ethanol (2) + 2-propanol (3) solvent mixture. [c]w_3 reflects the mass fraction of 2-MeTHF (3) in the binary ethanol (2) + 2-MeTHF (3) solvent mixture.[d]w_3 reflects the mass fraction of DMI (3) in the binary ethanol (2) + DMI (3) solvent mixture.

The correlation parameters and the ARD % of the modified Apelblat and Yaws equations in all biobased neat solvents and solvent mixtures are detailed in Table 6. The correlation parameters of the λh equation can be found in Table S8. The knowledge of these parameters allows the calculation of the TIM solubility at a specified temperature (T) in the studied neat and binary solvent mixtures. The low ARD % for the modified Apelblat (≤2.4689), Yaws (≤2.3793), and λh equations (≤4.7420) demonstrate that the experimentally determined solubility data correlated well using these model equations. The results for the correlations using the λh equation seem surprising considering the decomposition of TIM before the melting and, therefore, need to be assessed more carefully. The good correlations may indicate a minor effect of T_m of TIM on the accuracy of the λh model. This aspect could be proven by

calculating x^{cal}_1 of TIM at theoretical $T_{m,onset} \pm 20$ K and measured $\Delta H_{fus} = 476.79$ K. The comparison of the ARD % values resulted in nearly identical results (Figures S3 and S4 and Table S9).

Further comparing the data in Table 6 shows that the ARD % for the modified Apelblat and Yaws equations are very similar, with the modified Apelblat equation having slightly better correlations. The exceptions are Cyrene, DMI, 2MeTHF, and the binary solvent mixture ethanol (2) + 2- MeTHF (3) for $w_3 =$ 0.27 and $w_3 = 0.86$.

Figures 2 and 3 show the experimental and correlated mole fraction solubility of TIM (x_1) in the biobased neat solvents and binary solvent mixtures using the modified Apelblat equation. Diagrams illustrating the correlated solubility using the Yaws and λh models are displayed in Figures S5–S8. From Figures 2 and 3, it can be seen that the solubility of TIM increases with temperature (T) in all neat solvents and solvent mixtures. Moreover, Figure 3 shows that the temperaturedependent solubility of TIM in the biobased neat solvents decreases in the order: water > ethanol > Cyrene > acetone > 1-butanol > DMI > 2-propanol >2-MeTHF below 312 K. At temperatures above 312 K, the solubility order of TIM changes to water > ethanol > Cyrene > 1-butanol > acetone > DMI > 2-propanol > 2-MeTHF, representing a change of the solubility order for acetone and 1-butanol.

Figure 3.
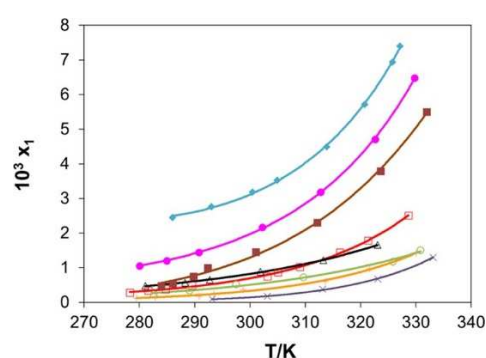
Experimental and correlated solubility data of TIM in biobased neat solvents: indigo tilted square solid, water; pink circle solid, ethanol; brown square solid, Cyrene; red square open, 1-butanol; △, acetone; green circle open, DMI; yellow +, 2-propanol; and purple ×, 2-MeTHF. The trendlines are calculated using the modified Apelblat equation. x_1 is the mole fraction solubility of TIM, while T is the temperature in Kelvin (K).

Since 2-propanol, 2-MeTHF, and DMI present low TIM solubility (Figure 3), they were chosen as potential antisolvents for the determination of TIM solubility in binary solvent mixtures with ethanol. Ethanol was chosen for the determination of solubility in binary solvent mixtures rather than water because it shows a stronger dependency of temperature on the solubility of TIM.

The surface plots in Figure 4 present the experimental and correlated mole fraction solubility (x_1) of TIM (1) using the modified Apelblat equation in the three binary solvent mixtures of ethanol (2) + 2-propanol (3), ethanol (2) + 2-MeTHF (3), and ethanol (2) + DMI (3). The surface plots generated by correlating the experimentally determined mole fraction solubility using the Yaws and λh equations can be found in

Figures S9 and S10, respectively. In Figure 4, the solubility of TIM in the binary solvent mixtures increases with increasing temperature. Additionally, the solubility of TIM decreases with increasing mass fraction of the antisolvent in the ethanol (2) + 2-propanol (3) and ethanol (2) + 2-MeTHF binary systems shown in Figure 4a,b, respectively. However, when 2-MeTHF is used as the antisolvent (Figure 4b), the solubility of TIM at lower temperatures (≤300 K) is not greatly altered by the antisolvent content below w_3 = 0.42. However, the impact increases with temperatures >300 K. Unlike 2-propanol and 2MeTHF, the presence of DMI in a binary solvent mixture with ethanol enhances the solubility of TIM (Figure 4c).

Specifically, the solubility of TIM in the binary solvent mixture of ethanol (2) + DMI (3) exceeds its solubility in either of the neat solvents, ethanol, and DMI for the temperature range studied. This demonstrates that DMI can act as a cosolvent for $w_3 \leq$ 0.70. Studying the root cause of the cosolvency effect of DMI goes beyond the scope of the study. Generally, cosolvency might be a result of the similarity between the solute and solvent molecules or preferential solvation of one of the solvents that leads to variations in solute–solvent interactions.[6,69,70]

Based on the data presented in Figure 4, it can be concluded that 2-propanol is superior as an antisolvent compared to 2MeTHF and DMI due to its enhanced impact on the solubility of TIM at all temperatures without cosolvency effects.

Figure 4.
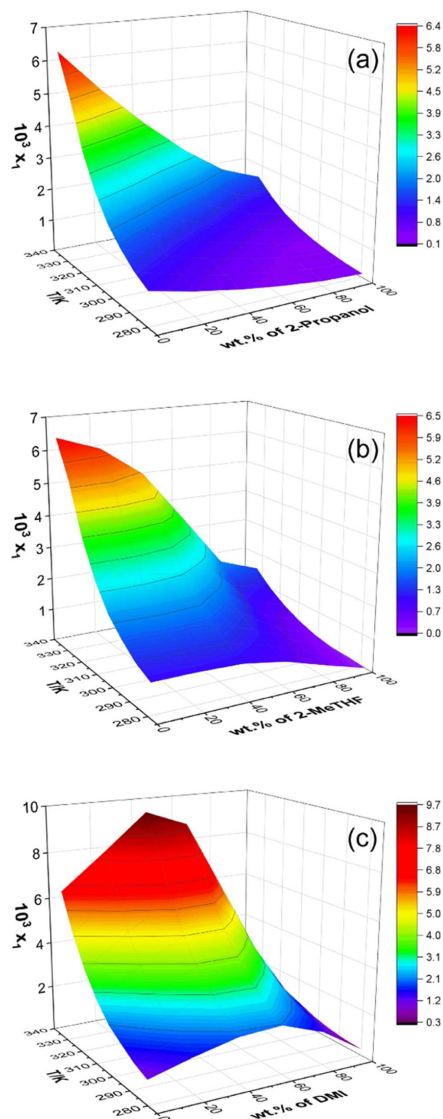
Surface plots showing the solubility of TIM (1) in binary solvent mixtures: (a) ethanol (2) + 2-propanol (3), (b) ethanol (2) + 2-MeTHF (3), and (c) ethanol (2) + DMI (3) correlated using the modified Apelblat equation. x_1 represents the mole fraction solubility of TIM, and T denotes the temperature in Kelvin (K).

ENANTIOMERIC PURITY ANALYSIS.

The enantiomeric purity of "as received" TIM and the solid material harvested after the completion of the solubility experiments by filtration were analyzed by HPLC (Figure S11 and Table S10).[46] The analysis reveals that the "as received" TIM is the pure *S*-enantiomer, (*S*)-TIM, with trace amounts (<0.1%) of the *R*-enantiomer, (*R*)-TIM, also known as the related compound A. The retention time for (*R*)- and (*S*)-TIM are about 9.5 and 13 min, respectively, demonstrating that they can be resolved

without any interference using the modified USP HPLC method in this study.[46] Moreover, Table S10 confirmed that all solids recovered from the suspensions via filtration for all neat and binary solvent mixtures were the commercial (*S*)-TIM with an enantiomeric purity of >99.7%.[46]

PXRD ANALYSIS.

TIM "as received" was analyzed prior to the solubility measurements, and the solid state was confirmed as the desired form of TIM (Figure S12).[29] After completion of the solubility measurements, all materials recovered from the suspensions via filtration were also characterized by PXRD. The PXRD analysis confirmed that the recrystallized material from all neat and binary solvent mixtures was the desired form of TIM (Figures S13–S16).[29]

Conclusions

The solubility data for TIM in eight biobased neat solvents and three binary biobased solvent mixtures was experimentally measured for the first time at temperatures between 278.15 and 333.15 K, except for acetone, which was between 278.15 and 323.15 K due to its low boiling point. All solubility data were determined using the polythermal method, with the exception of 2-MeTHF (the isothermal method was used). The experimental solubility data were correlated using the modified Apelblat, Yaws, and λh equations to provide a general quantification of the solubility curves for the estimation of TIM solubility at different temperatures in various neat solvents and solvent mixtures. The modified Apelblat and Yaws equations correlated well with the experimental solubility data demonstrated by the low ARD % values. The λh equation had higher ARD % values compared to the other two models, likely caused by the decomposition of TIM during melting, which alters the accuracy of the experimentally determined $T_{m,\,onset}$, needed in the equation. The experimental and correlated solubility data for biobased neat solvent and binary solvent mixtures presented in this study offer pathways for the development of more sustainable crystallization processes for TIM using renewable solvents.

ASSOCIATED CONTENT

SUPPORTING INFORMATION

The Supporting Information is available free of charge at https://pubs.acs.org/doi/10.1021/acs.jced.4c00060.

Detailed experimental procedure for the solubility curves of TIM in neat solvents and binary solvent mixtures; calculated surface plots of TIM in binary solvent mixtures using the Yaws and λh model equations, PXRD, DSC, and TGA thermographs. (PDF)

NOTES

The authors declare no competing financial interest.

NOMENCLATURE

A_i, B_i, C_i	empirical parameters for the modified Apelblat and Yaws equations
ARD %	average relative deviation
DMI	dimethyl isosorbide
DSC	differential scanning calorimeter
h	model parameter for the λh equation
HPLC	high-performance liquid chromatography
m	mass (g)
M	molecular mass (g·mol^{-1})
PXRD	powder X-ray diffraction
RD	relative deviation
T	absolute temperature (K)
T_{decomp}	decomposition temperature of the solute (K)
T_m	melting temperature of the solute (K)
TGA	thermogravimetric analysis
2-MeTHF	2-methyltetrahydrofuran
TIM	timolol maleate
u	standard uncertainty
w	mass fraction
x_i	mole fraction solubility of the solute (mol)

GREEK SYMBOLS

λ	parameter for the λh equation denoting the nonideal properties of the system

References

1. Gu, Y.; Jérôme, F. Bio-Based Solvents: An Emerging Generation of Fluids for the Design of Eco-Efficient Processes in Catalysis and Organic Chemistry. *Chem. Soc. Rev.* 2013, *42*, 9550–9570.

2. Brouwer, T.; Schuur, B. Dihydrolevoglucosenone (Cyrene), a Biobased Solvent for Liquid-Liquid Extraction Applications. *ACS Sustainable Chem. Eng.* 2020, *8*, 14807–14817.

3. Sharma, A.; Yu, E.; Morose, G.; Nguyen, D. T.; Chen, W. T. Designing Safer Solvents to Replace Methylene Chloride for Liquid Chromatography Applications Using Thin-Layer Chromatography as a Screening Tool. *Separations* 2021, *8*, 172.

4. Tseng, J. D.; Lee, H. L.; Yeh, K. L.; Lee, T. Recyclable Positive Azeotropes for the Purification of Curcumin with Optimum Purity and Solvent Capacity. *Chem. Eng. Res. Des.* 2022, *180*, 200–211.

5. Calvo-Flores, F. G.; Monteagudo-Arrebola, M. J.; Dobado, J. A.; Isac-García, J. Green and Bio-Based Solvents. *Top. Curr. Chem.* 2018, *376*, 18.

6. Myerson, A. S.; Erdemir, D.; Lee, A. Y. *Handbook of Industrial Crystallization*, 3rd ed.; Cambridge University Press: Cambridge, 2019.

7. Anastas, P. T.; Kirchhoff, M. M. Origins, Current Status, and Future Challenges of Green Chemistry. *Acc. Chem. Res.* 2002, *35*, 686–694.

8. NSF Engineering Research Visioning Alliance (ERVA). Engineering the Future of Distributed Manufacturing. https://www. ervacommunity.org/visioning-report/engineering-future-distributedmanufacturing/# (accessed December 03, 2023).

9. *Safeguarding the Bioeconomy*; National Academies Press: Washington, D.C., 2020.

10. European Union's Circular Economy Action Plan. https:// environment.ec.europa.eu/strategy/circular-economy-action-plan_en (accessed December 03, 2023).

11. Anastas, P. T.; Warner, J. C. Green Chemistry: Theory and Practice. In *Green Chemistry: Theory and Practice*; Oxford University Press: New York, 1998.

12. Brennecke, J. F. Green Engineering. *Green Chem.* 2004, *6*, 362. (13) García-Fernández, P. D.; Coto-Cid, J. M.; de Gonzalo, G. Green Oxidative Catalytic Processes for the Preparation of APIs and Precursors. *Catalysts* 2023, *13*, 638.

13. Silva-Brenes, D. V.; Emmanuel, N.; López Mejías, V.; Duconge, J.; Vlaar, C.; Stelzer, T.; Monbaliu, J. C. M. Out-Smarting Smart Drug Modafinil through Flow Chemistry†. *Green Chem.* 2022, *24*, 2094– 2103.

14. Wollensack, L.; Budzinski, K.; Backmann, J. Defossilization of Pharmaceutical Manufacturing. *Curr. Opin. Green Sustainable Chem.* 2022, *33*, No. 100586.

15. Jiménez-González, C.; Poechlauer, P.; Broxterman, Q. B.; Yang, B. S.; Am Ende, D.; Baird, J.; Bertsch, C.; Hannah, R. E.; Dell'Orco, P.; Noorman, H.; Yee, S.; Reintjens, R.; Wells, A.; Massonneau, V.; Manley, J. Key Green Engineering Research Areas for Sustainable Manufacturing: A Perspective from Pharmaceutical and Fine Chemicals Manufacturers. *Org. Process Res. Dev.* 2011, *15*, 900–911.

16. Monbaliu, J. C. M.; Stelzer, T.; Revalor, E.; Weeranoppanant, N.; Jensen, K. F.; Myerson, A. S. Compact and Integrated Approach for Advanced End-to-End Production, Purification, and Aqueous Formulation of Lidocaine Hydrochloride. *Org. Process Res. Dev.* 2016, *20* (20), 1347–1353.

17. Variankaval, N.; Cote, A. S.; Doherty, M. F. From Form to Function: Crystallization of Active Pharmaceutical Ingredients. *AIChE J.* 2008, *54*, 1682–1688.

18. López-Porfiri, P.; Gorgojo, P.; González-Miquel, M. Solubility Study and Thermodynamic Modelling of Succinic Acid and Fumaric Acid in Bio-Based Solvents. *J. Mol. Liq.* 2023, *369*, No. 120836.

19. Cañadas, R.; González-Miquel, M.; González, E. J.; Díaz, I.; Rodríguez, M. Evaluation of Bio-Based Solvents for Phenolic Acids Extraction from Aqueous Matrices. *J. Mol. Liq.* 2021, *338*, No. 116930.

20. Deng, D.; Han, G.; Jiang, Y.; Ai, N. Solubilities of Carbon Dioxide in Five Biobased Solvents. *J. Chem. Eng. Data* 2015, *60*, 104– 111.

21. World Health Organization. Model List of Essential Medicines 23rd List 2023 http://apps.who.int/bookorders.

22. Sambhara, D.; Aref, A. A. Glaucoma Management: Relative Value and Place in Therapy of Available Drug Treatments. *Ther. Adv. Chronic Dis.* 2014, *5*, 30–43.

23. Karhuvaara, S.; Kaila, T.; Huupponen, R. *β*-Adrenoceptor Antagonist Activities and Binding Affinities of Timolol Enantiomers in Rat Atria. *J. Pharm. Pharmacol.* 1989, *41*, 649–650.

24. DuBiner, H. B.; Hill, R.; Kaufman, H.; Keates, E. U.; Zimmerman, T. J.; Mandell, A. I.; Mundorf, T. K.; Bahr, R. L.;

25. Schwartz, L. W.; Towey, A. W.; Hurvitz, L. M.; Starita, R. J.; Sassani, J. W.; Ropo, A.; Gunn, R.; Stewart, W. C. Timolol Hemihydrate vs Timolol Maleate to Treat Ocular Hypertension and Open-Angle Glaucoma. *Am. J. Ophthalmol.* 1996, *121*, 522–528.

26. Mundorf, T. K.; Gate, E. A.; Sine, C. S.; Otero, D. W.; Stewart, J. A.; Stewart, W. C. The Safety and Efficacy of Switching Timolol Maleate 0.5% Solution to Timolol Hemihydrate 0.5% Solution Given Twice Daily. *J. Ocular Pharmacol. Ther.* 1998, *14*, 129–135.

27. Vioglio, P. C.; Chierotti, M. R.; Gobetto, R. Pharmaceutical Aspects of Salt and Cocrystal Forms of APIs and Characterization Challenges. *Adv. Drug Delivery Rev.* 2017, *117*, 86–110.

28. Gupta, D.; Bhatia, D.; Dave, V.; Sutariya, V.; Gupta, S. V. Salts of Therapeutic Agents: Chemical, Physicochemical, and Biological Considerations. *Molecules* 2018, *23*, 1719.

29. Bredikhin, A. A.; Bredikhina, Z. A.; Zakharychev, D. V.; Gubaidullin, A. T.; Fayzullin, R. R. Chiral Drug Timolol Maleate as a Continuous Solid Solution: Thermochemical and Single Crystal XRay Evidence. *CrystEngComm* 2012, *14*, 648–655.

30. Gaikwad, S. S.; Thombre, S. K.; Kale, Y. K.; Gondkar, S. B.; Darekar, A. B. Design and in Vitro Characterization of Buccoadhesive Tablets of Timolol Maleate. *Drug Dev. Ind. Pharm.* 2014, *40*, 680– 690.

31. Rathore, K. S.; Nema, R. K.; Sisodia, S. S. Timolol Maleate a Gold Standard Drug in Glaucoma Used as Ocular Films and Inserts: An Overview. *Int. J. Pharm. Sci. Rev. Res.* 2010, *3*, No. 005.

32. Kaemmerer, H.; Jones, M. J.; Lorenz, H.; Seidel-Morgenstern, A. Selective Crystallisation of a Chiral Compound-Forming SystemSolvent Screening, SLE Determination and Process Design. *Fluid Phase Equilib.* 2010, *296*, 192–205.

33. Reus, M. A.; Van Der Heijden, A. E. D. M.; Ter Horst, J. H. Solubility Determination from Clear Points upon Solvent Addition. *Org. Process Res. Dev.* 2015, *19*, 1004–1011.

34. Zorrilla-Veloz, R. I.; Stelzer, T.; López-Mejías, V. Measurement and Correlation of the Solubility of 5-Fluorouracil in Pure and Binary Solvents. *J. Chem. Eng. Data* 2018, *63*, 3809–3817.

35. George De La Rosa, M. V.; Santiago, R.; Malavé Romero, J.; Duconge, J.; Monbaliu, J. C.; López-Mejías, V.; Stelzer, T. Solubility Determination and Correlation of Warfarin Sodium 2-Propanol Solvate in Pure, Binary, and Ternary Solvent Mixtures. *J. Chem. Eng. Data* 2019, *64*, 1399–1413.

36. Marrero, V. R. V.; Berriós, C. P.; De Dios Rodríguez, L.; Stelzer, T.; López-Mejiás, V. In the Context of Polymorphism: Accurate Measurement, and Validation of Solubility Data. *Cryst. Growth Des.* 2019, *19*, 4101–4108.

37. Cruz, J. M. J.; Vlaar, C. P.; López-Mejías, V.; Stelzer, T. Solubility Measurements and Correlation of MBQ-167 in Neat and Binary Solvent Mixtures. *J. Chem. Eng. Data* 2021, *66*, 832–839.

38. FDA. Guidance for Industry. Q3C – Tables and List 2017 https://www.fda.gov/downloads/drugs/guidances/ucm073395.pdf (accessed September 25, 2023).

39. Camp, J. E.; Nyamini, S. B.; Scott, F. J. Correction: Cyrene Is a Green Alternative to DMSO as a Solvent for Antibacterial Drug Discovery against ESKAPE Pathogens. *RSC Med. Chem.* 2020, *11*, 317.

40. Yu, H.; Xue, Z.; Wang, Y.; Yan, C.; Chen, L.; Mu, T. Enabling Efficient Dissolution and Fractionation of Lignin by Renewable and Adjustable Dimethyl Isosorbide-Based Solvent Systems. *Sep. Purif. Technol.* 2023, *306*, No. 122688.

41. FDA. Q3C(R8) Impurities: Guidance for Residual Solvents Guidance for Industry 2021 https://www.fda.gov/vaccines-bloodbiologics/guidance-compliance-regulatory-information-biologics/biologics-guidances.

42. Wei, T.; Wang, C.; Du, S.; Wu, S.; Li, J.; Gong, J. Measurement and Correlation of the Solubility of Penicillin V Potassium in Ethanol + Water and 1-Butyl Alcohol + Water Systems. *J. Chem. Eng. Data* 2015, *60*, 112–117.

43. Pascual, G. K.; Donnellan, P.; Glennon, B.; Kamaraju, V. K.; Jones, R. C. Experimental and Modeling Studies on the Solubility of 2-Chloro-N-(4-Methylphenyl)Propanamide (S1) in Binary Ethyl Acetate + Hexane, Toluene + Hexane, Acetone + Hexane, and Butanone + Hexane Solvent Mixtures Using Polythermal Method. *J. Chem. Eng. Data* 2017, *62*, 3193–3205.

44. Sun, R.; He, H.; Wan, Y.; Wang, Y.; Li, L.; Sha, J.; Jiang, G.; Li, Y.; Li, T.; Ren, B. Solubility of Melatonin in Ethyl Acetate + (N, NDimethylformamide, 2-Methoxyethanol, 2-Ethoxyethanol and Methanol): Determination, Correlation, Thermodynamic Properties and Hansen Solubility Parameter at Saturation. *J. Chem. Thermodyn.* 2021, *156*, No. 106372.

45. Jia, Q.; Lei, D.; Zhang, S.; Zhang, J.; Liu, N.; Kou, K. Solubility Measurement and Correlation for HNIW·TNT Co-Crystal in Nine Pure Solvents from T = (283.15 to 318.15) K. *J. Mol. Liq.* 2021, *323*, No. 114592.

46. *Timolol Maleate Monograph*; United States Pharmacopeia and National Formulary, 2020.

47. Nyvlt́, J. Kinetics of Nucleation in Solutions. *J. Cryst. Growth* 1968, *3–4*, 377–383.

48. Smallwood, I. M. *Handbook of Organic Solvent Properties*; Arnold: London, Great Britain, 1996.

49. Vellema, J.; Hunfeld, N. G. M.; Van Den Akker, H. E. A.; Ter Horst, J. H. Avoiding Crystallization of Lorazepam during Infusion. *Eur. J. Pharm. Sci.* 2011, *44*, 621–626.

50. Tian, N.; Yu, C.; Du, S.; Lin, B.; Gao, Y.; Gao, Z. Solubility Measurement and Data Correlation of Isatoic Anhydride in 12 Pure Solvents at Temperatures from 288.15 to 328.15 K. *J. Chem. Eng. Data* 2020, *65*, 2044–2052.

51. Yu, C.; Chen, M.; Lin, B.; Tian, N.; Gao, Y.; Wu, S. Solubility Measurement and Data Correlation of 5,5-Dimethylhydantoin in 12 Pure Solvents at Temperatures from 283.15 to 323.15 K. *J. Chem. Eng. Data* 2020, *65*, 814–820.

52. Wang, X.; Qin, Y.; Zhang, T.; Tang, W.; Ma, B.; Gong, J. Measurement and Correlation of Solubility of Azithromycin Monohydrate in Five Pure Solvents. *J. Chem. Eng. Data* 2014, *59*, 784–791.

53. Guo, Y.; Yin, Q.; Hao, H.; Zhang, M.; Bao, Y.; Hou, B.; Chen, W.; Zhang, H.; Cong, W. Measurement and Correlation of Solubility and Dissolution Thermodynamic Properties of Furan-2-Carboxylic Acid in Pure and Binary Solvents. *J. Chem. Eng. Data* 2014, *59*, 1326– 1333.

54. Yan, H.; Wang, Z.; Wang, J. Correlation of Solubility and Prediction of the Mixing Properties of Capsaicin in Different Pure Solvents. *Ind. Eng. Chem. Res.* 2012, *51*, 2808–2813.

55. Yaws, C. L. *Chemical Properties Handbook: Physical, Thermodynamic, Environmental, Transport, Safety, and Health Related Properties for Organic and Inorganic Chemicals*; McGraw-Hill: New York, 1999.

56. Xue, M.; Huang, D.; Yang, K.; Chen, L.; Zheng, Z.; Xiang, Y.; Huang, Q.; Wang, J. Measurement, Correlation of Solubility and Thermodynamic Properties Analysis of 2,4,6-Trinitroresorcinol Hydrate in Pure and Binary Solvents. *J. Mol. Liq.* 2021, *330*, No. 115639.

57. Ma, M.; Wang, J.; Yang, X.; Zhao, Z. Determination and Simulation of the Solubility of Bifonazole in 14 Pure Solvents at 283.15–323.15 K. *J. Chem. Eng. Data* 2023, *68*, 1748–1762.

58. Liu, D.; Hu, S.; Zhao, Y.; Wang, Y.; Zhang, S.; Wang, J.; Wang, J.; Wang, P.; Li, Z. Solubility and Polymorphism of a HOF Monomer N1,N3,N5-Tris(Pyridin-4-Yl)Benzene-1,3,5-Tricarboxamide in 12 Neat Solvents at Temperatures from 283.15 to 323.15 K. *J. Chem. Eng. Data* 2023, *68*, 1244–1252.

59. Wang, P.; Guo, Y.; He, H.; Huang, H.; Qiu, J.; Han, J.; Hu, S.; Liu, H.; Zhao, Y. Solubility Determination and Thermodynamic Modeling of N-Acetylglycine in Different Solvent Systems. *J. Chem. Eng. Data* 2021, *66*, 1344–1355.

60. Zhou, L.; Zou, C.; Wang, M.; Li, L. Solubility of Hydroxyl Cucurbit[6]Uril in Different Binary Solvents. *J. Chem. Eng. Data* 2014, *59*, 2879–2884.

61. Buchowski, H.; Ksiazczak, A.; Pletrzyk, S. *Solvent Activity along a Saturation Line and Solubility of Hydrogen-Bonding Solids*; ACS, 1980; Vol. *84*.

62. Dwyer, L.; Kulkarni, S.; Ruelas, L.; Myerson, A. Two-Stage Crystallizer Design for High Loading of Poorly Water-Soluble Pharmaceuticals in Porous Silica Matrices. *Crystals* 2017, *7*, 131.

63. Roa Engel, C. A.; ter Horst, J. H.; Pieterse, M.; van der Wielen, L. A. M.; Straathof, A. J. J. Solubility of Fumaric Acid and Its Monosodium Salt. *Ind. Eng. Chem. Res.* 2013, *52*, 9454–9460.

64. European Pharmacopoeia. *General Notices*, 2010.

65. Gabbott, P. *Principles and Applications of Thermal Analysis*; Blackwell Publishing Ltd.: Iowa, 2008.

66. Abdelaziz, A.; Zaitsau, D. H.; Mukhametzyanov, T. A.; Solomonov, B. N.; Cebe, P.; Verevkin, S. P.; Schick, C. Melting Temperature and Heat of Fusion of Cytosine Revealed from Fast Scanning Calorimetry. *Thermochim. Acta* 2017, *657*, 47–55.

67. Ford, J. L.; Mann, T. E. Fast-Scan DSC and Its Role in Pharmaceutical Physical Form Characterisation and Selection. *Adv. Drug Delivery Rev.* 2012, *64*, 422–430.

68. Cebe, P.; Thomas, D.; Merfeld, J.; Partlow, B. P.; Kaplan, D. L.; Alamo, R. G.; Wurm, A.; Zhuravlev, E.; Schick, C. Heat of Fusion of Polymer Crystals by Fast Scanning Calorimetry. *Polymer* 2017, *126*, 240–247.

69. Jouyban, A. Review of the Cosolvency Models for Predicting Solubility of Drugs in Water-Cosolvent Mixtures. *J. Pharm. Pharm. Sci.* 2008, *11*, 32–58.

70. Zhu, G.; Wang, N.; Huang, X.; Wang, T.; Zhou, L.; Hao, H. Reveal the Molecular Mechanism of Cosolvency Behaviors of Proline in Alcohol + Acetone Binary Mixed Solvent. *J. Ind. Eng. Chem.* 2024, *132*, 172–181.